Neurobiology of Disease 130 (2019) 104519

Contents lists available at ScienceDirect

Neurobiology of Disease

journal homepage: www.elsevier.com/locate/ynbdi

Small-molecule drug screening identifies drug Ro 31-8220 that reduces toxic phosphorylated tau in *Drosophila melanogaster*

Kyu-Ho Shim[a,b,1], Soo-Hwan Kim[a,b,1], Joon Hur[a,b,1], Dong-Hou Kim[a,b], Atanas Vladimirov Demirev[c,**], Seung-Yong Yoon[a,b,*]

[a] Department of Brain Science, Asan Medical Center, University of Ulsan College of Medicine, Seoul, Republic of Korea
[b] Bio-Medical Institute of Technology (BMIT), University of Ulsan College of Medicine, Seoul, Republic of Korea
[c] Korea University, Republic of Korea

ARTICLE INFO

Keywords:
Ro 31-8220
Neurodegeneration
Tau
Phosphorylated tau
Kinase inhibition
Frontotemporal dementia

ABSTRACT

The intraneuronal aggregates of hyperphosphorylated and misfolded tau (neurofibrillary tangles, NFTs) cause a stereotypical spatiotemporal Alzheimer's disease (AD) progression that correlates with the severity of the associated cognitive decline. Kinase activity contributes to the balance between neuron survival and cell death. Hyperactivation of kinases including the conventional protein kinase C (PKC) is a defective molecular event accompanying associative memory loss, tau phosphorylation, and progression of AD or related neurodegenerative diseases. Here, we investigated the ability of small therapeutic compounds (a custom library) to improve tau-induced rough-eye phenotype in a *Drosophila melanogaster* model of frontotemporal dementia. We also assessed the tau phosphorylation in vivo and selected hit compounds. Among the potential hits, we investigated Ro 31-8220, described earlier as a potent PKCα inhibitor. Ro 31-8220 robustly improved the rough-eye phenotype, reduced phosphorylated tau species in vitro and in vivo, reversed tau-induced memory impairment, and improved the fly motor functions. In a human neuroblastoma cell line, Ro 31-8220 reduced the PKC activity and the tau phosphorylation pattern, but we also have to acknowledge the compound's wide range of biological activity. Nevertheless, Ro 31-8220 is a novel therapeutic mitigator of tau-induced neurotoxicity.

1. Introduction

Paired helical microtubule-associated protein tau filaments (insoluble aggregates) are the hallmark of several neurodegenerative diseases, including frontotemporal dementia (FTD) and Alzheimer's Disease (AD). Current treatments for FTD and AD provide only modest symptomatic relief. Genetic mutations in tau are the leading causes of neurodegeneration in FTD, but the underlying mechanisms triggered by specific mutations remain mostly unknown (Colodner and Feany, 2010; Wittmann et al., 2001). Numerous types of kinases have been linked to hyperphosphorylated tau species. Cyclin-dependent protein kinase-5 (CDK5) is able to induce increasing tau phosphorylation and neurodegeneration (Patrick et al., 1999). P38 (Feijoo et al., 2005), extracellular signal-regulated kinase 1/2 (Erk1/2) (Ekinci and Shea, 1999; Guise et al., 2001), and c-Jun N-terminal kinases (JNK) (Reynolds et al., 1997) phosphorylate tau at various sites in AD patients brains. Tau-tubulin kinase 1/2 dose-dependently induce tau phosphorylation (Tomizawa et al., 2001) and casein kinase 1/2 also phosphorylate tau in AD brains (Greenwood et al., 1994). Microtubule affinity-regulating kinase (MARK) and glycogen synthase (GSK)-3β (Shulman and Feany, 2003; Trinczek et al., 2004). Protein kinase C (PKC) both directly phosphorylates tau (Correas et al., 1992) and indirectly causes the dephosphorylation of tau by phosphorylating and inactivating GSK-3β (Isagawa et al., 2000). Genetic screening of tauopathy modulators in a *Drosophila melanogaster* model showed that multiple kinases and phosphatases contribute to the phosphorylation of human tau and tau-associated neurotoxicity (Shulman and Feany, 2003). However, a later study demonstrated that changes in tau phosphorylation state are not required to suppress or enhance its toxicity in FTD fly model (Ambegaokar and Jackson, 2011). Nevertheless, targeting tau

* Correspondence to: S.-Y. Yoon, Alzheimer's Disease Experts Lab (ADEL), Department of Brain Science, University of Ulsan College of Medicine, 88, Olympic-ro 43-gil, Songpa-Gu, Seoul 05505, Republic of Korea.
** Correspondence to: Atanas V. Demirev, Department of Microbiology, College of Medicine, Korea University, 73 Inchon-Ro, Seongbuk-gu, Seoul, Republic of Korea.
E-mail addresses: avdemirev@korea.ac.kr (A.V. Demirev), ysy@amc.seoul.kr (S.-Y. Yoon).
[1] These authors contributed equally.

https://doi.org/10.1016/j.nbd.2019.104519
Received 11 July 2018; Received in revised form 13 May 2019; Accepted 20 June 2019
Available online 22 June 2019

phosphorylation through inhibition of protein kinases could represent a valid therapeutic approach to reducing tau aggregation and associated neuronal death (Churcher, 2006; Hanger et al., 2009).

Drug repositioning involves two main approaches: first approach isutilizing the mechanism of action that is already licensed for a specific drug (Ashburn and Thor, 2004) and second approach is aiming to identify novel targets for existing active chemicals. Most directly, we can use the second approach and identify bioavailable compounds for clinical use against neurodegeneration by in vivo screening with whole-animal tau-induced neurotoxicity models. In the past decade, the vinegar fly, *D. melanogaster,* has emerged as a highly efficient model system to study neurodegeneration in vivo (Marsh and Thompson, 2006; Pandey and Nichols, 2011). We can efficiently recapitulate FTD- or AD-causing genetic mutations and use *D. melanogaster* as a valuable drug testing platform for neurodegeneration research (Pandey and Nichols, 2011). Abnormal phosphorylation of tau have been successfully observed in the fruit fly glial cells (Colodner and Feany, 2010; Wittmann et al., 2001). Tau have been shown to produce the neurotoxicity and a rough-eye phenotype when expressed in the fruit fly retina (via GMR promoter) (Jackson et al., 2002; Nishimura et al., 2004; Wittmann et al., 2001). Karsten et al. (Karsten et al., 2006) successfully used the same FTD *Drosophila* model (Jackson et al., 2002) to identify suppressors of tau-induced neurodegeneration, and we also used it in our primary screening (Material and Methods '*D. melanogaster* rough-eye phenotype') to detect any improvements of the rough-eye phenotype upon drug administration. The rough-eye phenotype consists of a reduction in eye size and a loss of the usual ommatidial arrangement, which reflects underlying neurodegeneration, neuronal loss, and disorganization of the retina (Jackson et al., 2002). Mild to severe rough-eye phenotypes are easily assessable by three single, independent mutations in human tau transgene (P301L (Jackson et al., 2002; Karsten et al., 2006), V337M (Dias-Santagata et al., 2007), and R406W (Khurana et al., 2006; Wittmann et al., 2001)), related to familial FTD.

This research aimed to specifically use tau^{P301L} and tau^{R406W} as models of tau-induced neurotoxicity (familial FTD) in *D. melanogaster* and to screen a custom collection of small active molecules (Table S1) for their ability to ameliorate tau-induced neurotoxicity in vivo and to study the mechanisms underlying the compound activity. We identified Ro 31–8220 (Han et al., 2000) as a potential novel drug candidate to ameliorate tau-induced neurotoxicity in *D. melanogaster* and to recover tau-induced memory impairment and loss of motor function. Ro 31-8220, also known as bisindolylmaleimide-IX (Bis-IX or BIM-IX) (Beltman et al., 1996; Bit et al., 1993), directly inhibits conventional PKC. As a cell-permeable lipophilic chemical, Ro 31-8220 enters cells through passive diffusion, and its activity has been tested in various types of cells, including platelets and T lymphocytes (Mayati et al., 2015; Mayati et al., 2017; Standaert et al., 1999), revealing that Ro 31-8220 targets multiple cellular mechanisms such as autophagy (Ouseph et al., 2015) and apoptosis (Begemann et al., 1998; Han et al., 2000). In low doses, it could be beneficial for cell survival (Hemstrom et al., 2005). In this study, we investigated Ro 31-8220 potential to modulate tau-induced neurotoxicity in a fly model of FTD.

2. Materials and methods

2.1. Chemical reagents

We used 120 pharmacologically active compounds, listed in the pharmaceutical inventory list at the Department of Brain Science, Asan Medical Center, with a broad range of cell signaling activities. We dissolved each drug, including Ro 31-8220 mesylate (TOCRIS Cat. No.2002, 10 mg) in 30% dimethyl sulfoxide (DMSO, 5 mM stock solution). Then, we diluted the stock solutions to 250 μM using sterile distilled water and mixed it with fresh standard fly food to produce a working concentration of 20 μM. The standard fly food was replaced with fresh drug-supplemented food every 2–3 days. We used DMSO-containing standard fly food (0.03–0.06%) as a control.

2.2. Transgenic fly stocks and maintenance

The transgenic flies were regularly grown and maintained at 25 °C and 60% humidity on a 12 h light–dark cycle and a standard cornmeal medium (recipe by Bloomington Drosophila Stock Centre, [BDSC], Bloomington, Indiana, USA). We obtained *D. melanogaster elav*^{c155}-*GAL4* (#25750) and *gl-htau*^{P301L} (#51377, (Jackson et al., 2002)) lines from BDSC. *UAS-htau*^{WT} and *UAS-htau*^{R406W} were kind gifts from Dr. Mel Feany, MA, USA (Khurana et al., 2006; Wittmann et al., 2001). We generated pUAS-tau^{P301L} expression plasmid by cloning human tau2N4R containing P301L mutation into a p5xUAS-MCS-attB plasmid, which was derived from pKC26 vector (6 kb, VDRC). BestGene Inc. (MA, USA) generated the tau-transgenic flies (*UAS-htau2N4R*^{P301L}) by insertion at the *attP* site in the *VIE260B* genetic background, a fly line used to generate the VDRC-KK collection (#60100, VDRC (Dietzl et al., 2007)). We backcrossed *all lines* for at least five generations to a w^{1118} line (#60000, VRDC), which is a well-known fly control line with normal circadian rhythm, learning, and memory.

2.3. D. melanogaster rough-eye phenotype

Virgin female flies (*gl-tau*^{P301L}, #51377, BDSC) were collected and crossed to W1118 (VDRC) males. Up to 50 age-matched larvae (3–5 days post-egg-laying) containing *gl-tau*^{P301L} genotype were collected and grown in standard cornmeal food containing the selected active compound at 25 °C. We collected male progeny 5–10 d PE and assessed light stereomicroscope images of their eyes for any improvement of the rough-eye phenotype, captured using an 8.1 MP color digital camera (Sony, DSC-W90 Cyber-Shot). We analyzed the fly eye images in ImageJ (imagej.nih.gov) and calculated the eye size. The fold-change ratio shows a comparison of at least six independent tau rough-eye phenotype images (produced after administration of a selected drug) with six images of tau-expressing flies fed with control solvent solution. We assessed the significance of changes, using a volcano plot, as the calculated *p*-values and against the fold changes in fly eye size in GraphPad Prism 6 (GraphPad Software, Inc., La Jolla, CA).

2.4. Volcano plot analysis of the rough-eye phenotype

No conventional path has been established for false discovery rates, and currently, the cut-off for a statistical significance in experimental volcano plots are mostly chosen manually. We customized a volcano plot in order to visualize our selection process, where we calculated -log10 [p-value] and log [fold change] of the eye size (eye volume) for each chemical producing a phenotype. After plotting the data, we defined a lower middle quadrant, where the eye phenotype is in a range of expected variance (± 0.35, i.e., exhibiting no significant variance from the control). With this approach, we were targeting the right upper square in the volcano plot for true positive hits. In testing for a rough-eye phenotype change, we divided the chemicals into two groups (in order to ease our screening protocol). Group 1 consisted of 57 compounds (3 compounds were excluded due to insufficient quantities prior to testing) produced more robust phenotypes, and the fold change data are displayed in Table S1. Visual observation of the eye phenotypes and assessment on the volcano plots showed us that we should establish a more stringent pattern between ± 0.05 (log [fold change]) (which was chosen as our base threshold). We choose a cut-off value for the –log10 [p-value] of 0.58 because with this threshold compounds such as GSK-3β inhibitor, pyruvate, and insulin appeared in the lower middle quadrant, which correlated with our observations, where the eye volume did not increase significantly. We found that compounds like GSK-3β inhibitor and pyruvate produced a positive change at the first trial but did not show a robust improvement of the rough-eye phenotype in the second and third independent tests (Table S2 and S3).

Table 1
Characteristics of medial temporal gyrus human brain samples.

Source	Sex	Age (years)	Braak	PMD(hh:mm)	Weight(g)
AD patient	M	85	5	07:10	1020
AD patient	M	70	6	04:50	1040
AD patient	M	87	5	06:10	1047
AD patient	M	65	6	08:50	1057
normal control	M	87	1	10:20	1256
normal control	M	80	0	07:15	1331
normal control	M	84	1	05:35	1337
normal control	M	78	1	17:40	1125

The brain extracts were from four Alzheimer's disease (AD) patients and four age- and sex-matched controls (see Materials and Methods). We displayed the tissue preparation time after death as postmortem delay (PMD). A topographic staging of the neurofibrillary tangles (NFTs) diagnosed the AD pathology, as described by (Braak and Braak, 1991) - 5 or 6 in AD cases and 0 or 1 in control brains.

2.5. Antibodies

Rabbit anti-Phospho-tau Ser199/202 (44-768, 1:1000), rabbit anti-Phospho-tau Ser262 (44-750, 1:1000), rabbit anti-Phospho-tau Ser396 (44–752, 1:1000), and mouse anti-phospho-tau Th181 (AT270, MN1050, 1:1000) were purchased from Invitrogen. Rabbit anti-phospho-tau Ser214 (ab170892, 1:1000) was from Abcam. Rabbit anti-Phospho-(Ser) PKC substrate antibody was from Cell Signaling (#2261, 1:1000). Rabbit anti-HA was from Roche. Tau5 (MAB3420, 1:1000) was from Calbiochem. Mouse anti-actin antibody, clone C4 (MAB1501, Chemicon) was more specific in flies and was used in the control immunoblots from *Drosophila melanogaster* head extracts; β-actin (A5441, 1:10,000, Sigma) was engaged in the rest of the experiments.

2.6. Human brain tissues and APP/PS1-Tg mouse brain tissue

In this study, we used medial temporal gyri specimens from four AD patients (obtained from the Netherlands Brain Bank, Table 1) and four age- and sex-matched controls. AD pathological staging was based on the Braak staging system (Braak and Braak, 1991). We analyzed the mouse cortical tissue from APP/PS1 and age-matched (6 months old) control mice by Western blot analysis for total phosphorylated substrates of protein kinase C (PKC).

2.7. Cell culture, transfection, and drug treatment

SH-SY5Y cells were cultured in Dulbecco's Modified Eagle's Medium (DMEM, Hyclone) with 10% fetal bovine serum. All cells were cultured in a 5% CO_2 atmosphere at 37 °C. Plasmids containing hemagglutinin-tagged tau (tau.P301L::HA and tau.WT::HA, pcDNA5 vector) were transfected into human neuroblastoma (SH-SY5Y) or HeLa cells using Lipofectamine 2000 (Invitrogen, #11668–019), according to the manufacturer's guidelines, and incubated for 24 h. For drug treatment, we incubated the cells in fresh media containing 0, 0.5, 1, or 5 μM Ro 31–8220. After 24 h of incubation, we lysed the transfected cells in lysis buffer (50 mM Tris-HCl, 250 mM NaCl, 0.1% NP-40, 1% Triton X-100, and 10% glycerol at pH 7.3) containing a phosphatase and protease inhibitor mix (Sigma). Extracts were centrifuged at 13,000 rpm for 10 min at 4 °C. We performed all Western blots according to general methods.

2.8. D. melanogaster survival assay

elav^{c155}*-Gal4* virgins were collected, sorted into batches of 50–100 flies, and crossed with age-matched males to produce the desired genotypes. At least 120 male flies per genotype (expressing one copy of *tau* transgene) were collected at 0–1 d PE and aged on standard cornmeal food (Bloomington recipe) complemented with 1.0% agar. Each vial (9.5 × 2.4 cm) was kept on its side at 25 °C and 60% humidity under a 12 h light–dark cycle. The number of flies per vial was optimized to 25 to avoid any mortality unrelated to phenotype. We exchanged the fly food (containing drug) every 2–3 days and collected and counted the dead flies. We analyzed the differences in survival using the Kaplan–Meier equation in GraphPad Prism 6 (GraphPad Software, Inc., La Jolla, CA).

2.9. Negative geotaxis assay

We assessed the climbing behavior in a clean 15 cm high × 2.4 cm diameter polystyrene vial. Male flies (23–25 per vial) were collected 0–1 d PE and transferred without anesthesia, given 30–60 s of rest before and between trials, and gently tapped to the bottom in a dark room under a red light (Paterson Safelight Photax Filter, SH2013011, UK). We calculated means ± standard errors of the mean (SEM) of six independent experimental fly cohorts tested serially every 5 d within 50 d from d 0–1 PE. We calculated the climbing activity by counting the number of flies above a mark on the vial at 5 cm, 10 s after tapping the vial, and we expressed the values as a percentage of the number of flies in the vial. Images (videos) were taken using a Sony DSC-90 Cyber-shot 8.1 camera placed and leveled 40 cm in front of the test vial.

2.10. Learning and memory assay

We used a two-choice, Y-maze conditioned preference test for an odor associated with ethanol, as described by (Kaun et al., 2011). Briefly, we collected up to 18 groups (10–12 male flies/group) of a single genotype 0–1 d PE, reared at 25 °C, and tested them at 25 d PE. We trained the flies in a 15 × 15 × 15 cm chamber. Humidified air was bubbled through 53% ethanol (*v*/v) at a flow rate of 1.5 L·min^{-1} at 24 °C to produce alcohol vapor entering the training chamber. For the Y-maze data assessment, we calculated the preference index (PI) for the odor paired with ethanol (conditioned stimulus, CS) as (number of flies in the paired-odor arm – the number of flies in the unpaired-odor arm)/(total number of flies). Then, we calculated a conditional preference index (CPI) for conditioned odor preference or conditioned odor aversion by averaging the preference indices for reciprocally trained groups of flies. We performed control tests as previously described (Kaun et al., 2011). In additional control odor preference assessments, we tested the tau expressing flies by allowing them to choose between a single odor in the first arm of the Y-maze and air in the second arm. In the control experiments, all fly genotypes showed no preference at 20, 30, and 35 days PE.

2.11. Statistical analysis

We performed statistical analyses using one-way ANOVA with Bonferroni correction or unpaired Student's *t*-tests. All values are expressed as the means ± SEM of at least three independent experiments.

3. Results

We performed drug screening, where first we tested 120 active compounds (a costumed library, designed for identifying modulators of neurodegeneration) for improvement of rough-eye phenotype (*gl-tau*^{P301L} flies) and second, we examined the phosphorylation of human mutant tau when expressed in the fly CNS (*elav-Gal4* > *UAS-tau*^{P301L} transgenic animals), grown on food containing a specified chemical (20 μM). Human tau [0N4R] transgenic fly lines, where tau is ectopically expressed in *Drosophila* larval eye discs under glass-responsive enhancer (Freeman, 1996; Ollmann et al., 2000) produce an abnormal eye phenotype upon eclosion (i.e., *gl-tau*^{P301L} transgenic flies, (Jackson et al., 2002)). Crossing transgenic fly lines containing tau phosphorylation mutants (downstream of upstream activating sequence, UAS (Brand and Perrimon, 1993)) to an *elav-Gal4* driver (Robinow and

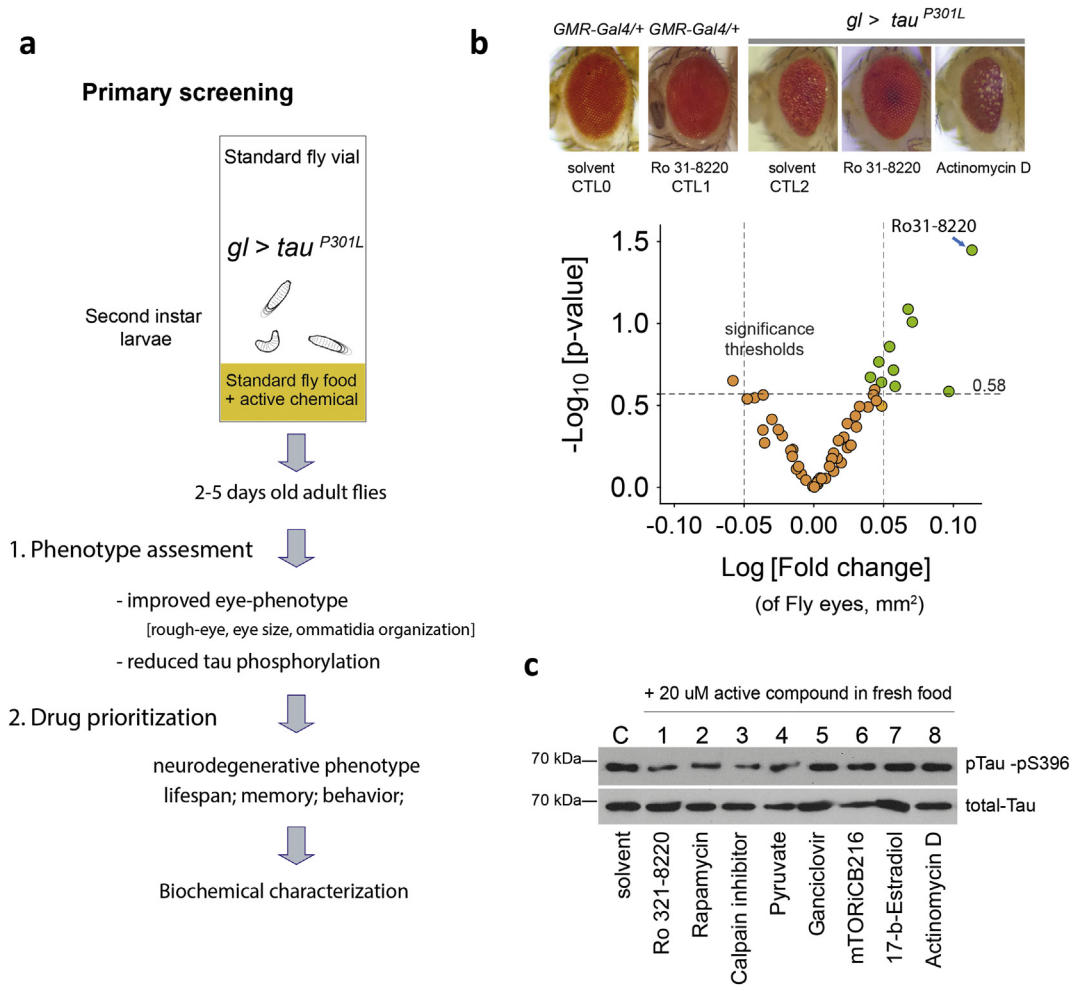

Fig. 1. Ro 31-8220, a potent bioactive chemical against tauopathy in vivo. (a) Screening paradigm in a *D. melanogaster* model of tauopathy; Primary drug screening: we prioritized the active substances according to improvement in the rough-eye phenotype (eye size, more organized ommatidia, (b) and a Western blot detection of phosphorylated tau species (c). In the primary screening, we crossed virgin female flies carrying *gl-tau*^{P301L} with male flies wild white eye (w1118). We fed 3-day-old larvae food containing 20 μM active compound (a). Adult male flies with the desired genotype (*gl-tau*^{P301L}) were collected at day 0 post-eclosion (d PE) and examined for the neurodegenerative (rough-eye) phenotype 4–7 d PE. A customized volcano plot (b) exhibits the process of drug prioritization using $\log_{-10}$ of the *p*-value against log of the fold change in fly eye size (volume, mm^2), where the cut-off values -log10[p-value] = 0.58 and log[fold change (eye-size, mm^2)] were assigned to reduce the false positive values (see Material and methods). Ro 31-8220 produced the most significant improvements in compound eye volume and ommatidia (b lower panel, and Fig. S1), compared with *gl-tau*^{P301L} flies control flies grown on standard fly food supplemented only with the solvent plus DMSO. In (b), *gl-tau*^{P301L} flies fed with actinomycin D-containing food served as a negative control, as actinomycin D enhanced the neurodegeneration (severe rough-eye phenotype and eye-size reduction). (c) in the second step of the screening we used a Western Blot analysis of phosphorylated human tau at pS396 and compared the results with the rough-eye phenotype assessment in the first step (b); (c) represents an example of the drug selection by Western Blot, where four of the selected drugs, displayed here (including Ro 31–8220 and three other known active compounds), decreased tau phosphorylation. We used flies expressing tau^{P301L} in the CNS (*elav*^{c155}*-Gal4 > tau*^{P301L}). Ro 31–8220 produced robust results in both steps of the screening.

White, 1988) induces ectopic gene expression in the fly CNS at all developmental stages and could be used to detect changes of tau-phosphorylation in head extracts from transgenic tau^{P301L} flies (i.e., *elav*^{c155}*-Gal4 > UAS-tau*^{P301L}) grown on food supplemented with a specific drug. A fly line was not commercially available; therefore, we generated UAS-tau^{P301L} transgenic flies by inserting human tau2N4R^{P301L} (Material and Methods) into a modified p5xUAS-attB vector, used previously for generation of the RNAi-KK library at VDRC (Vissers et al., 2016). The transgene was placed after a 5xUAS sequence and inserted at a specific attP site in the fly genome.

First, we fed 3-day-old *gl-tau*^{P301L} fly larvae with a single drug (Fig. 1a) and monitored the treated animals after eclosion, looking for an improvement in the rough-eye phenotype. We separated the 120-drug library into two groups of 60 compounds to perform the screening. We collected at least 60 male flies from three independent drug treatments and assessed the eye phenotype under a microscope. In order to visualize the fold changes in the eye phenotype, we plotted the log [fold change of the *gl-tau*^{P301L} fly eye's volume] against the –$\log_{10}$ [the *P*-values] for each drug tested (Fig. 1a). At the first screening trial, we identified 18 positive hits (from both groups) that improved the rough-eye phenotype (Table S2). We observed that 8 drugs in group 2 (63 compounds) showed improved rough-eye phenotype on the first drug treatment (Table S2) but exhibited no significant alteration on the second and third drug trial (all positives from the triplicate in Table S3). The three independent treatments minimized the false positives and reduced the hit compounds to only 10 (Table S3). The compounds in group 1 (n = 57) produced a more robust rough-eye phenotype in triplicate testing. Since group 1 included all the 10 positive hits, we used this data to represent our screening process (Table S1 and volcano plot on Fig. 1b). Three compounds were excluded from group 1 due to isufficinet quantities prior to the testing. The visual assessment of the eye phenotypes revealed that a substantial portion of the drugs did not significantly alter the *Drosophila* eye size or ommatidia arrangement. Only 8% of 120 compounds significantly increased the eye volume and

improved the organization of the ommatidia (Fig. S1b, Table S3), while 12.5% produced a slight improvement of the rough-eye phenotype compared to the controls (Fig. S1a and b). Four percent of the 120 compounds aggravated the neurodegenerative phenotype (Table S1, mifepristone, actinomycin D, geldanamycin, and BIX01294; Fig. 1b left at the volcano plot), producing severely fused ommatidia and reduced eye volume (i.e., the negative phenotype observed for actinomycin D; Fig. 1b and Fig. S1c). Four percent exhibited toxicity during the larvae treatment, and the *gl-tau*^{P301L} animals did not survive.

The rough-eye phenotype did not always correlate with tau phosphorylation (Ambegaokar and Jackson, 2011). Therefore, we also tested if the drugs could reduce human tau phosphorylation when tau^{P301L} is expressed in the fly CNS (*elav*^{c155}*-Gal4 > UAS-tau*^{P301L}, Fig. 1c). Although tau is found mainly in the neuronal axon and soma, previous work suggested that tau is missorted and accumulated at the synapses under pathological conditions (Hoover et al., 2010). The PHF-1 epitope with Ser396 phosphorylation is well characterized in studies of neurodegeneration. Chronic stress stimuli also results in a significant accumulation of cytosolic total tau as well as increases levels of Thr231-, Ser262-, and Ser396/404-tau phospho-epitopes at the synapses (Lopes et al., 2016). We tested several commercially available antibodies against these three epitopes with head protein extracts from tau^{P301L} flies (*elav*^{c155}*-Gal4 > UAS-tau*^{P301L}) in order to detect reduction in phosphorylated tau as a second step in the drug screening. We found that pS202, pS262, and pThr231, were giving somewhat fluctuating results in tau^{P301L} flies and the phosphorylated tau bands were often absent (data not shown). This resonated with previous publication in mouse model where epitopes such as pS202 and pS231 (i.e. AT8 and AT180, respectively) that showed decreased immunoreactivity in tau^{P301L} mice (Terwel et al., 2005). pS396 is highly conserved tau phosphorylation site, and readily detectable in *Drosophila* models of tau-induced neurotoxicity ((Papanikolopoulou and Skoulakis, 2015) and this study). Early phosphorylation on Ser396 preceding learning and memory deficits and neurodegeneration have also been reported in a mouse AD model (Kanno et al., 2014) and we also proceeded our screening with detection of pS396 in tau^{P301L} flies.

In both screening steps, five days post-eclosion (d PE) the male transgenic flies were collected, the eye-phenotypes were assessed (*gl-tau*^{P301L}), and the head protein extracts (*elav*^{c155}*-Gal4 > UAS-tau*^{P301L}) were examined for a reduction in tau phosphorylation. This provided a robust primary platform for our investigation (Fig. 1a). Three independent protein extracts from fly heads (*elav*^{c155}*-Gal4 > UAS-tau*^{P301L}) (three heads per active compound) were tested to determine whether the administered drugs could mitigate tau phosphorylation. Seven active compounds produced a reduction in tau phosphorylation at pS396 (rapamycin, Ro 31-8220, calpain inhibitor, pyruvate, P3075, isoliquiritigenin, and taxol; Fig. 1b, Fig. S1d, and S1d'), but they could be selected for the next step only if the same drug also produced an improvement of the rough-eye phenotype (Fig. 1a and b). Compounds, such as ouabain and ganciclovir (involved in another study at our institution) slightly improved the rough-eye phenotype but did not reduce tau phosphorylation (Fig. 1Sb and Table S1). In contrast, pyruvate and P3075 reduced the tau phosphorylation at pS693 but improved the rough-eye phenotype only in the first drug screening trial (Table S2). We concluded the screening with the identification of 10 hit compounds (Fig. 1A, labeled in green, and Fig. S1b) producing improvement in the rough-eye phenotype and 7 compounds inducing a reduction of tau-phosphorylation (Fig. 1c; Fig. S1d). Hit compounds, such as rapamycin (mTOR-inhibitor) (Ozcelik et al., 2013; Talboom et al., 2015) and calpain inhibitor (a tau C-terminal cutting enzyme) (Nikkel et al., 2012), which produce beneficial eye phenotype changes and reduced tau phosphorylation, are already known to inhibit tau-induced neurodegeneration. However, our drug prioritization showed one novel candidate, Ro 31-8220, that substantially improved the ommatidium arrangement (Fig. 1b), produced the largest compound eye volume (compared to the controls; Fig. 1a, Table S1), and also reduced tau phosphorylation at pS396 (Fig. 1c). Initially Ro 31-8220 was identified as a potent PKCα inhibitor, also known as BIM-IX (Beltman et al., 1996; Bit et al., 1993) but later was shown to have multiple target mechanisms (Mayati et al., 2015; Standaert et al., 1999), and at higher doses it could contribute to apoptosis in cancer cells (Han et al., 2000). Our data asserted Ro 31-8220 as an interesting candidate for further in vivo testing of its effects on neurodegenerative phenotypes in *Drosophila* models of tau-induced neurodegeneration.

Supporting a role for enhanced signaling by PKC in AD, a recent phosphoproteomics study of postmortem human brains identified increased phosphorylation of PKC substrates as an early event in AD (Tagawa et al., 2015). Anti-phospho-PKC substrate antibody (p-PKC substrates) targeting sequence (R/K)XS(hydrophobic)(R/K) (Cell Signaling #2261) has been frequently used to examine the phosphorylation activity by conventional PKCs (cPKC), PKCα (Jensen et al., 2009; Pierchala et al., 2004; Thomassen et al., 2011). We have to acknowledge that this antibody could recognize multiple peptides with phosphorylated Ser/Thr proceeded by Arg or Lys residues, which are targeted by AGC-group protein kinases (Pearce et al., 2010), but it also effectively detects conventional PKC activation (Okamoto and Shikano, 2017) or inhibition (Pierchala et al., 2004) in vitro. We examined the conventional PKC activity in cortex samples from human AD patients (Fig. 2a, Table 1) and APP/PS1 mouse brains (Fig. 2b) using this anti-phospho-PKC substrate antibody. Although we could not directly measure PKC activity from tissue, we found an increase in multiple substrate phosphorylation, suggesting PKC/kinase activation in the brain extracts of AD patients as well as in APP/PS1 mouse brains. A human neuroblastoma cell line (SH-SY5Y) incubated in the presence of 1 and 5 μM of Ro 31-8220 produced a reduction in PKC substrate phosphorylation (Fig. 3a). Most importantly, the phosphorylation of tau also showed a significant reduction at specific positions, such as pS396, pS202, and pS262 (Fig. 3b) in cells transiently expressing two isoforms of human tau (tau2N4R^{WT} and tau2N4R^{P301L}), incubated in the presence of 1 and 5 μM of Ro 31–8220. This again could refer to conventional PKC inhibition; it may also refer to other kinases as potential targets for Ro 31–8220 activity.

Next, we tested the ability of Ro 31-8220 to ameliorate neurodegeneration in flies. We expressed human tau in the fly central nervous systems (CNS) (by *elav*^{c155}*-Gal4* driver (Lin and Goodman, 1994)) and grew 3-day-old larvae on a standard fly food supplemented with 20 μM Ro 31-8220 (Fig. 1a). In the initial test, the expression of UAS-tau^{P301L} (generated in this study) by *elav*^{c155}*-Gal4* did not sufficiently shorten the fly's lifespan or impair the fruit fly's memory compared to controls (flies were tested until age 50 d PE, data not shown). We assumed these transgenic flies produced low tau expression in fly CNS, plausibly due to 5xUAS or other positional effects. The lower expression levels were effective for testing the in vivo tau phosphorylation (Fig. 1c) but not efficient for the following neurodegenerative behavior tests (Fig. S3). Therefore, we overexpressed wild-type and R406W-mutated isoforms of human tau (a kind gift from Feany M. MD. Ph.D. (Wittmann et al., 2001)) in fly CNS (*elav*^{c155}*-Gal4 > UAS-tau*^{R406W}). After the metamorphosis, we selected males with the desired genotype (i.e., *tau*^{R406W}) and continued the treatment of the flies on a standard fly food supplemented with Ro 31–8220. The lifespan of flies fed with Ro 31-8220 as a supplement (> 200 males; Fig. 4a, *tau*^{R406W} - Ro 31-8220 flies) was significantly improved, compared to the control fly group (*tau*^{R406W} flies) grown on food containing only the solvent. Tau^{R406W} male flies that received 20 μM Ro 31-8220 also showed enhanced locomotor abilities 35 and 40 days after eclosion, as seen in Fig. 4b and b'.

Twenty- to thirty-day-old males with the designated genotype, tau^{WT}, and tau^{R406W}, grown on food containing only the control solvent (Fig. 4d), showed alcohol-induced olfactory memory impairment. All fly genotypes were trained with two consecutive exposures to odorants, where the second odorant was conditioned with 53% ethanol vapors (Fig. 4c), as previously reported (Kaun et al., 2011). We added a 5 min flow of humidified air between the two odorant exposures (Fig. 4c), as

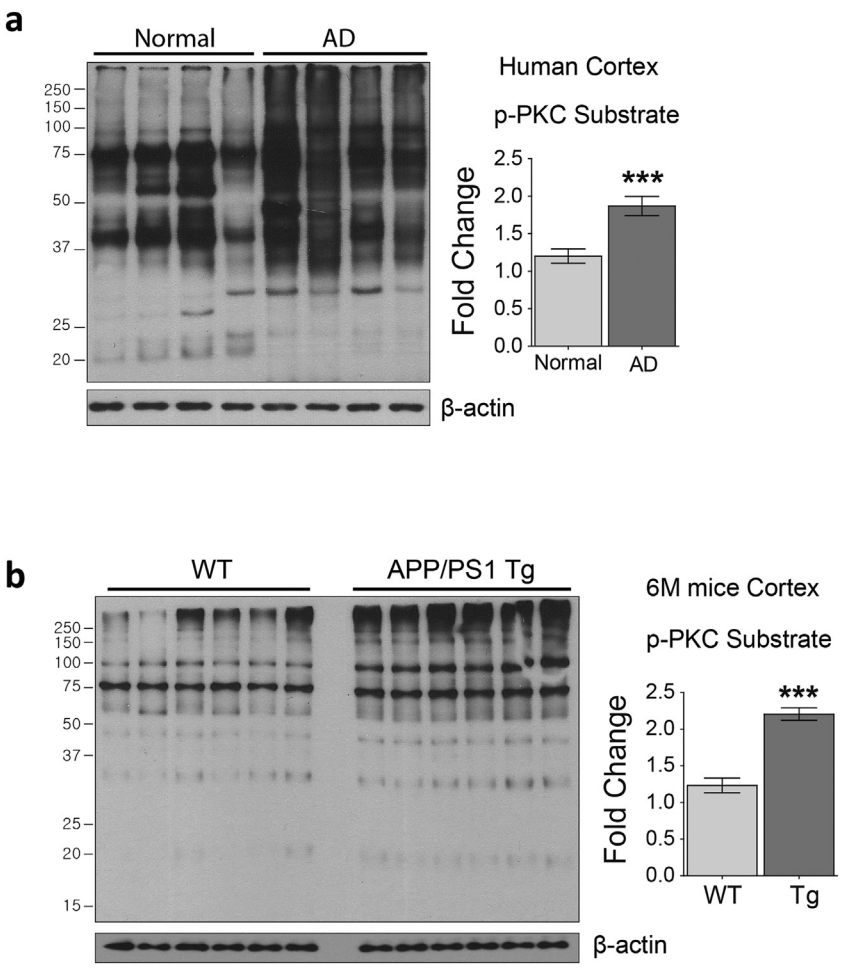

Fig. 2. PKC activity in cortex samples from AD human patients (a) and APP/PS1 mouse model of AD disease (b). Brain extracts from the medial temporal gyri of four AD patients and four age- and sex-matched controls (described in Table 1) were subjected to immunoblot analysis for anti-phosphorylated PKC substrates (CS #2261). The antibody recognizes a broad spectrum of peptide targets (Pearce et al., 2010) but also effectively detects conventional PKC activation (Okamoto and Shikano, 2017) or inhibition (Pierchala et al., 2004) in vitro. (b) Protein extracts from the cortices of APP/PS1 Tg mice also exhibited increased PKC activity. The quantifications (calculated using ImageJ) in (a) and (b) only indirectly represent the increased activity of conventional PKC in neurodegenerative brains; Student's *t*-test, $***P < 0.001$.

we found this to improve the fly conditioning. The alcohol conditioning produced aversive behavior in control wild-type flies 20–120 min after the training and attractive behavior 24 h after the training. Ro 31–8220-treated *elav*^{c155}*-Gal4* > *tau*^{R406W} flies showed consistent improvement of alcohol-induced memory (in three consecutive assays) compared to the control *elav*^{c155}*-Gal4* > *tau*^{R406W} flies. Flies expressing the wild-type human tau by *elav*^{c155}*-Gal4* (tau^{WT} flies) also exhibited shorter lifespans and impaired motor functions (Fig. S1) when treated only with the drug solvent. Treatment with Ro 31–8220 (tau^{WT} (Ro 31–8220)) did not seem to significantly improve longevity (Fig. S1a), but male flies exhibited enhanced climbing abilities (Fig. S1b) and improved ethanol-conditioned olfactory memory (Fig. S1d) compared to control flies.

In recent study, analysis showed an activation of the PKCα signaling pathway, which resulted in earlier tau phosphorylation at pSer214. Fujita et al. (2018) demonstrated that depletion of progranulin in an animal model of frontotemporal lobar degeneration produced an increase in tau phosphorylation at pSer214, tau mislocalization to dendritic spines, and a synaptic loss (Fujita et al., 2018). Administration of a PKC inhibitor reversed the tau phosphorylation, improved the dendritic spines' integrity, and reduced spine loss (Fujita et al., 2018). We asked whether phosphorylation at pSer214 could be affected in the FTD model we used for behavior tests. We found that brain extracts from *elav*^{c155}*-Gal4* > *tau*^{R406W} flies grown on a standard food supplemented with 20 μM Ro 31–8220 showed markedly reduced phosphorylation at pS214 (Fig. 5). In contrast, the pS214 in fly brain extracts containing the normal human tau isoform did not decrease, and we concluded that the phosphorylation of wild-type tau at this position was unaffected by the drug treatment. This could reflect lower toxicity and better solubility of the wild-type tau compared with the familial R406W FTD mutant isoform. We also found that phosphorylation of tau at other specific positions (pSer396 and pThr181) was significantly decreased in both models. All quantifications were normalized against the total tau (tau5). The reduction of tau phosphorylation at multiple amino acid residues in brain extracts from tau-expressing flies might denote Ro 31–8220 targeting multiple kinases and reducing the neurotoxic effect of tau in the *Drosophila* brain.

4. Discussion

Whole-genome sequencing has identified mutations that cause overactivation of PKCα in late-onset AD patients (Alfonso et al., 2016). Clinical trials have suggested that cancer therapy should focus on activating PKC, rather than inhibiting it (Mochly-Rosen et al., 2012). A meta-analysis of nine independent studies revealed that AD patients have a decreased risk of developing cancer compared with the general population, which is consistent with reports that AD and cancer display an inverse association (Shi et al., 2015). Considering these opposing roles of conventional PKC in cancer and AD, repurposing PKC inhibitors for the treatment of Late-onset Alzheimer's disease (LOAD) may prevent the effects of toxic protein accumulation on synapses and thereby mitigate the loss of cognitive function. Identified as a PKC alpha modulator, a β-branching polyketide compound bryostatin-1 has been administered in pre-clinical trials involving AD patients (Nelson et al., 2017). Loss of PKC function has been shown to be associated with cancer (Mochly-Rosen et al., 2012), but its enhanced activity has also been correlated with neurodegeneration (Shi et al., 2015). Three independent mutations in PKCα identified in patients with late-onset AD

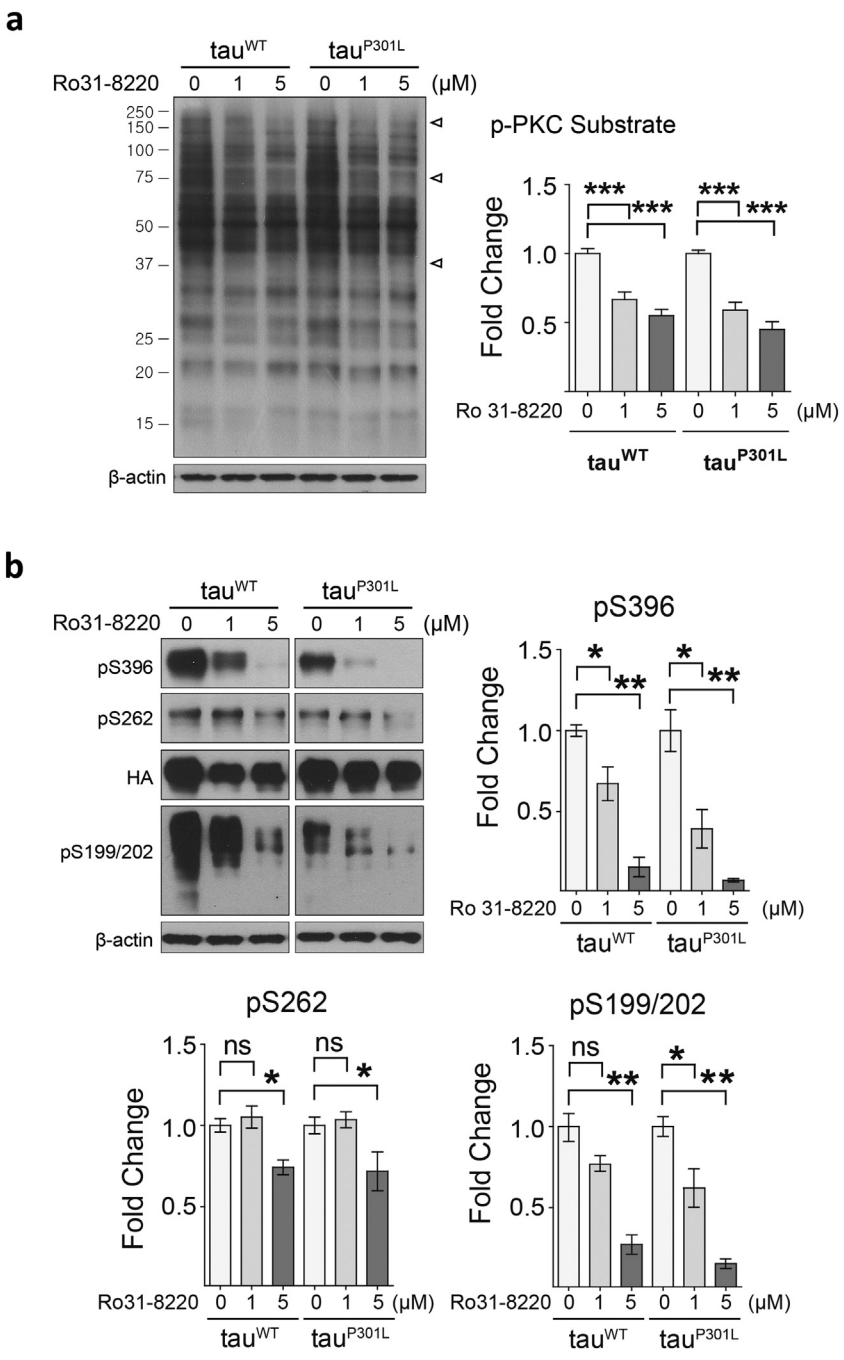

Fig. 3. Ro 31–8220 inhibits PKC activity in human neuroblastoma cells (SH-SY5Y) and decreases the phosphorylation of tau in vitro. SH-SY5Y cells were transiently expressing two human tau isoforms and incubated in complete culture media supplemented with 1 and 5 μM Ro 31-8220. (a) Reduction in multiple phosphorylated PKC substrates can be observed in the presence of 1 and 5 μM Ro 31-8220. Arrowheads show specific areas with decreased phosphorylation; the phosphoprotein intensity was quantified and normalized against actin (on the right). (b) Phosphorylated-tau at positions pSer396, pSer262, and pSer199/202 consistently reduced in SH-SY5Y cells, transiently expressing human tau2N4R (wild-type and P301L isoforms) in the presence of 1 and 5 μM Ro 31–8220. The protein intensity was normalized against the total tau represented by hemagglutinin (HA) staining. The analysis showed that Ro 31-8220 produces a decrease from three independent experiments, $^{*}P < 0.05$, $^{**}P < 0.01$, ***P < 0.001.

were shown to increase catalytic activity, which correlated with reduced synaptic activity, potentially accelerating disease progression (Alfonso et al., 2016). This abnormal PKC activity is an intriguing potential mechanism to explore in AD treatment research. Indeed, (Hoshi et al., 2010) found that synaptic plasticity improved after treatment of rat brain slices with a PKC inhibitor (BisIV). Through the reduction of toxic PKCα (Lucke-Wold et al., 2015) and activation of PKCε, bryostatin-1 induces growth of mature synapses, prevents neuronal death, and influences amyloid plaques and tau tangles (Nelson et al., 2017). Bryostatin-1 facilitated the translocation and downregulation of not only PKCα but also PKCβ in NIH 3 T3 fibroblast cells (Szallasi et al., 1994). However, the effects of bryostatin-1 treatment stem from initial activation of PKCα, and then a subsequent reduction in phosphorylated PKC substrates (Ab – cell signaling), plausibly a result of proteasome degradation and gene down-regulation as a compensatory mechanism (Pierchala et al., 2004).

Here, we approached the neurodegenerative disease from a phenotypic standpoint by screening for chemical modulators of tau-induced neurodegeneration (rather than isolated cells or proteins) in a *D. melanogaster* model of FTD. We identified a novel drug candidate for the treatment of tau-induced neurodegeneration, Ro 31-8220, a well-known inhibitor of conventional PKCα (BIM-IX (Beltman et al., 1996; Bit et al., 1993; Mayati et al., 2015; Standaert et al., 1999)). Direct inhibition or activation of processes downstream of PKC, p70S6K, Msk1, or p90Rsk using Ro 31–8220 have been a valuable tool for investigating various physiological, pathological, and pharmacological cellular regulatory pathways (Cuenda and Alessi, 2000). In addition to PKC inhibition, pretreatment with Ro 31–8220 (1–2 μM) could inhibit the phospholipase Cγ2 (PLCγ2) phosphorylation accompanying platelet aggregation (stimulated by amyloid β, 10 μM) (Shen et al., 2008). Reports of the PKC-independent off-target effects highlight the lack of specificity of Ro 31–8220 (Mayati et al., 2015; Standaert et al., 1999).

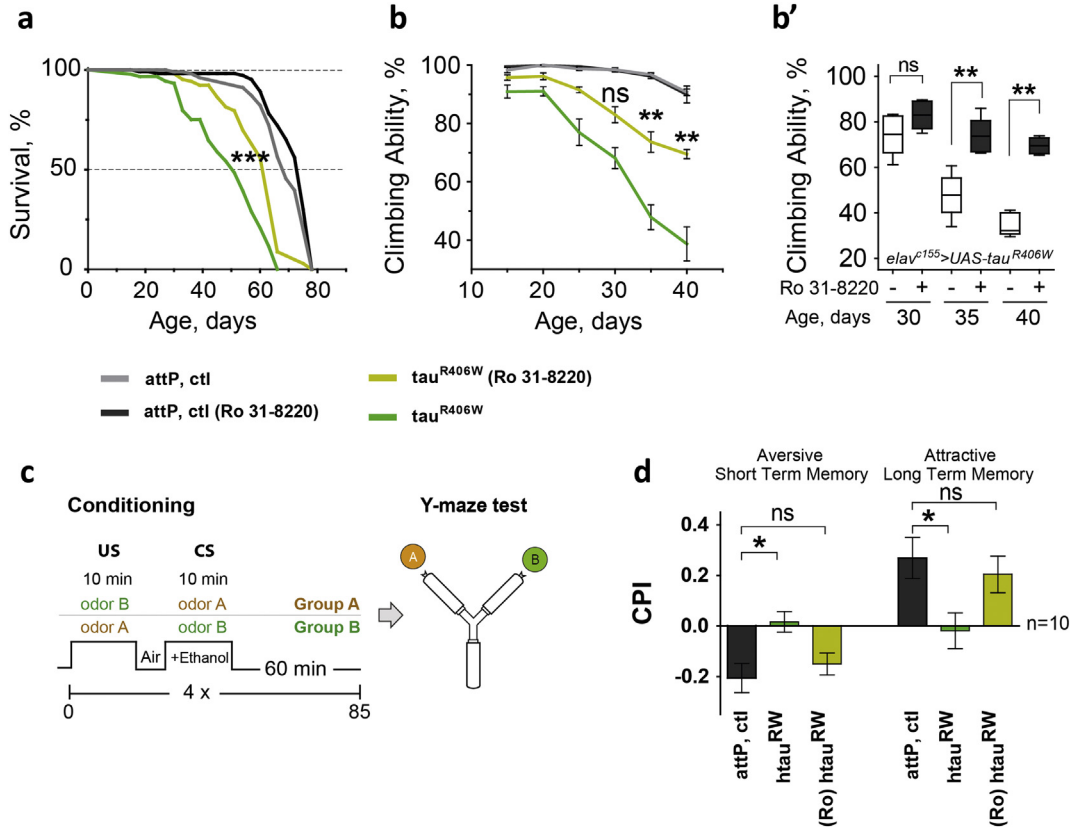

Fig. 4. Administration of Ro 31-8220 improves the neurodegenerative behavior of *elav^{c155}-Gal4 > tau^{R406W}* flies. (a) The longevity assay: *elav^{c155}-Gal4 > tau^{R406W}* flies had significantly longer lifespans following Ro 31-8220 administration. (b and b') show the tau-flies' climbing abilities; Ro 31-8220 administration improved the performance of adult males 35 and 40 days post-eclosion (PE). (c) Spaced ethanol-conditioned memory training scheme: We administered three spaced training sessions of a 10 min exposure to a first odor (odor A), followed by a 5 min exposure to humidified air, then a 10 min exposure to a second odor (odor B) paired with 53% ethanol vapor. The flies chose between the two arms of a Y-maze containing different odors (odor A or odor B). (d) Ethanol-conditioned memory assay in flies expressing tau^{R406W}: *elav^{c155}-Gal4 > tau^{R406W}* male flies showed impaired attractive (30–60 min after training) and aversive (24 h after training) memory at age 25–30 d PE. The flies expressing tau^{R406W} regained their memory after Ro 31–8220 administration [tau^{R406W} (Ro 31-8220)]. We incubated all genotypes on standard fly food supplemented with Ro 31-8220 (20 μM) or control solvent solution (0.05% dimethyl sulfoxide [DMSO]). All genotypes were under the *elav^{c155}-Gal4* driver. Statistical analysis was by one-way analysis of variance (ANOVA) with Bonferroni correction. attP, ctl – male flies with genotype elav^{c155}-Gal4 > attP, where attP derives from a control fly line with w1118, attP, *VIE260B* (VDRC) genetic background used for transgene insertions (Dietzl et al., 2007)], US – unconditioned stimulus, CS – conditioned stimulus, CPI – conditional preference index.

Ro 31–8220 notably inhibits mitogen-activated protein kinase (MAPK) phosphatase-1 (Yeo et al., 1997); the RSK1, RSK2, and RSK3 isoforms of p90 ribosomal S6 kinase; p70 ribosomal S6 kinase; CDC2 histone H1 kinase; and glycogen synthase kinase-3 (Mayati et al., 2015). It also activates phosphoinositide phospholipase C (Beltman et al., 1996) and c-Jun N-terminal kinase (Standaert et al., 1999), induces apoptosis in cancer cells, and blocks voltage-dependent sodium channels in a PKC-independent manner. In contrast to staurosporine (Davis et al., 1989; Han et al., 2000) (a broad-range PKC inhibitor that activates apoptotic machinery in non-small cell lung carcinoma (Joseph et al., 2002)), its derivative analog Ro 31-8220 decreases phorbol-12-myristate-13-acetate-induced ERK phosphorylation and suppresses Akt phosphorylation (Hemstrom et al., 2005), which results in reduced apoptotic events. Our findings assert Ro 31-8220 as an exciting target for further investigation in FTD and LOAD treatment. We observed that concentrations as low as 1 μM in mammalian cell cultures and < 50 μM as a food supplement for fruit fly models of tauopathy were beneficial and reduced the tau phosphorylation at several amino acid residues, reversed memory deficits, and improved tau-induced neurodegenerative behavior. Bisindolylmaleimides (BIMs), such as Ro 31-8220, could directly inhibit the activity of the ABC transporter P-glycoprotein (ABCB1) (Mayati et al., 2017), a critical glial component of the blood–brain barrier (BBB) beneficial in a drug delivery platform. BIMs also block the activity of breast cancer resistance protein (BCRP/ABCG2), an ATP efflux pump also involved in anticancer drug resistance, as well as ABCB1, which is the leading protein involved in BBB drug resistance (Robey et al., 2007). These examples of the activation or inhibition of multiple pathways support the notion that, in low doses, we can utilize Ro 31–8220 as a supplement with other drugs to treat FTD and LOAD. Further investigation is required to elucidate additional pathways that involve Ro 31-8220.

5. Conclusions

Our study highlights the therapeutic potential of Ro 31–8220 for the reduction of tau-phosphorylation and tau-induced neurodegeneration in vivo. We have a pronounced need for practical pharmacological interventions against protein-misfolding neurodegenerative disorders, such as AD and FTD, which are increasing in prevalence but have no effective treatment. Recent studies have highlighted the strong conservation in signaling pathways from flies to humans, which enables the cross-reactivity of 'human' drugs in flies and the capacity of drugs to be efficacious in fly larvae and adult fruit flies when ingested with their food (Agrawal et al., 2005; Aritakula and Ramasamy, 2008; Edwards et al., 2011; Kang et al., 2002; McBride et al., 2005). Cellular signaling that underlies the initiation and progression of neurodegenerative diseases unearths potential targets for therapeutic interventions. The genomes of individuals with familial LOAD showed three rare

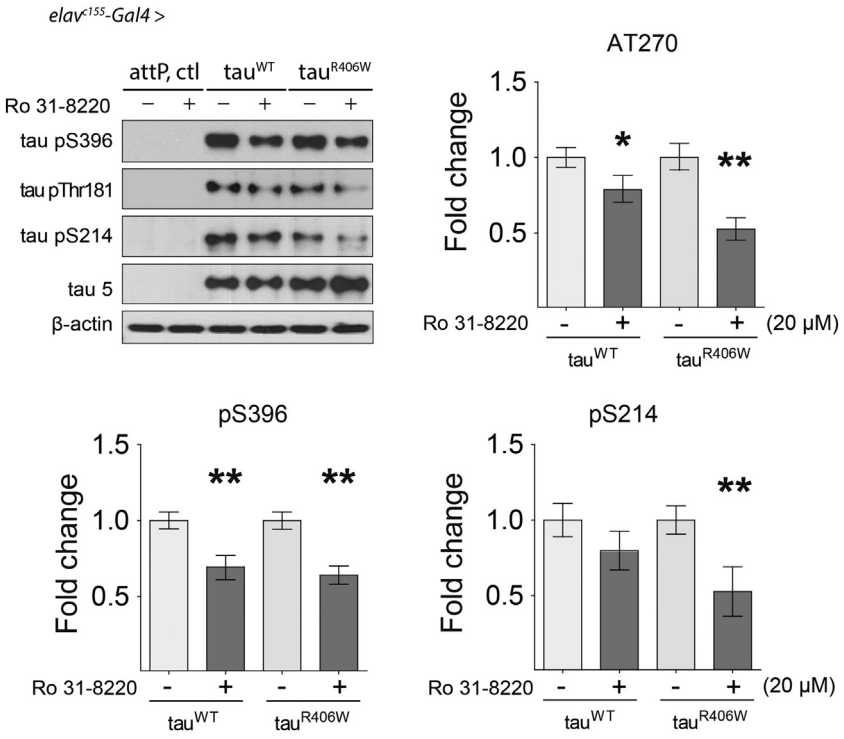

Fig. 5. Reduction of phosphorylated tau in brain extracts from a *D. melanogaster* model of tauopathy observed after Ro 31-8220 administration. We tested the brain extracts from 20- to 25-day-old flies fed with Ro 31-8220 at 25–27 °C. We expressed two human tau isoforms tau^{WT} and tau^{R406W} under $elav^{c155}$-*Gal4* (the pan-neuronal central nervous system [CNS] driver). Specific antibodies against phosphorylated tau at positions pS396, pS214, and pThr181 showed decreased affinities for flies fed with 20 μM Ro 31-8220 as a food supplement. The reduction of tau phosphorylation in $elav^{c155} > tau^{R406W}$ fly head extracts was more significant than in tau^{WT} flies, which could be reflecting lower tau^{WT} toxicity. The graphs in the figure show the quantified changes from 3 independent brain extracts per genotype. All quantifications were normalized against the total tau (tau5). Statistical analysis was by one-way analysis of variance (ANOVA) with Bonferroni correction.

mutations of PKCα with aberrant signaling outputs relative to wild-type PKCα (Alfonso et al., 2016), supporting the hypothesis that enhanced PKCα signaling may contribute to AD pathogenesis. Along with the activation of c-Jun in an in vitro study, Ro 31–8220 exhibits the most potent and direct inhibitory activity against PKCα (Beltman et al., 1996). Our data support the hypothesis that the phosphorylation of mutant tau and its neurotoxicity can be reduced by administering Ro 31–8220. A balanced inhibition or activation of conventional enzymes could be targeted for LOAD prevention and therapy early in the disease course.

Author contributions

S-H.K. and J H. collected the male flies imaged, analyzed the eye phenotypes, and were actively involved in the screening. A.V.D. designed and managed the project. K-H.S. and A.V.D. performed the Western blot analysis and the fly behavior assessments. A.V.D. and S.Y.Y. revised the paper. All authors provided critique and approved the submission.

Acknowledgments

We thank the Netherlands Brain Bank for providing human brain materials. We also thank the brain donors and their relatives for making these neuropathological studies possible. We are very grateful to Prof. Mel Feany M.D., Ph.D. Boston, MA, USA, for the kind gift of UAS-human wild-type and R406W tau fly lines. This work was supported by the Basic Science Research Program, through the National Research Foundation (NRF) of Korea, funded by the Ministry of Science, ICT & Future Planning (2018R1A2A1A05077403) and by MRC grant funded by the Korean government (MSIT) (2018R1A5A2020732).

Declaration of Competing Interests

The authors report no financial interests or potential conflicts of interests.

Appendix A. Supplementary data

Supplementary data to this article can be found online at https://doi.org/10.1016/j.nbd.2019.104519.

References

Agrawal, N., et al., 2005. Identification of combinatorial drug regimens for treatment of Huntington's disease using Drosophila. Proc. Natl. Acad. Sci. U. S. A. 102, 3777–3781.
Alfonso, S.I., et al., 2016. Gain-of-function mutations in protein kinase Calpha (PKCalpha) may promote synaptic defects in Alzheimer's disease. Sci. Signal. 9, ra47.
Ambegaokar, S.S., Jackson, G.R., 2011. Functional genomic screen and network analysis reveal novel modifiers of tauopathy dissociated from tau phosphorylation. Hum. Mol. Genet. 20, 4947–4977.
Aritakula, A., Ramasamy, A., 2008. Drosophila-based in vivo assay for the validation of inhibitors of the epidermal growth factor receptor/Ras pathway. J. Biosci. 33, 731–742.
Ashburn, T.T., Thor, K.B., 2004. Drug repositioning: identifying and developing new uses for existing drugs. Nat. Rev. Drug Discov. 3, 673–683.
Begemann, M., et al., 1998. Growth inhibition induced by Ro 31-8220 and calphostin C in human glioblastoma cell lines is associated with apoptosis and inhibition of CDC2 kinase. Anticancer Res. 18, 3139–3152.
Beltman, J., et al., 1996. The selective protein kinase C inhibitor, Ro-31-8220, inhibits mitogen-activated protein kinase phosphatase-1 (MKP-1) expression, induces c-Jun expression, and activates Jun N-terminal kinase. J. Biol. Chem. 271, 27018–27024.
Bit, R.A., et al., 1993. Inhibitors of protein kinase C. 3. Potent and highly selective bisindolylmaleimides by conformational restriction. J. Med. Chem. 36, 21–29.
Braak, H., Braak, E., 1991. Neuropathological stageing of Alzheimer-related changes. Acta Neuropathol. 82, 239–259.
Brand, A.H., Perrimon, N., 1993. Targeted gene expression as a means of altering cell fates and generating dominant phenotypes. Development 118, 401–415.
Churcher, I., 2006. Tau therapeutic strategies for the treatment of Alzheimer's disease. Curr. Top. Med. Chem. 6, 579–595.
Colodner, K.J., Feany, M.B., 2010. Glial fibrillary tangles and JAK/STAT-mediated glial and neuronal cell death in a Drosophila model of glial tauopathy. J. Neurosci. 30, 16102–16113.
Correas, I., et al., 1992. Microtubule-associated protein tau is phosphorylated by protein kinase C on its tubulin binding domain. J. Biol. Chem. 267, 15721–15728.
Cuenda, A., Alessi, D.R., 2000. Use of kinase inhibitors to dissect signaling pathways. Methods Mol. Biol. 99, 161–175.
Davis, P.D., et al., 1989. Potent selective inhibitors of protein kinase C. FEBS Lett. 259, 61–63.
Dias-Santagata, D., et al., 2007. Oxidative stress mediates tau-induced neurodegeneration in Drosophila. J. Clin. Invest. 117, 236–245.
Dietzl, G., et al., 2007. A genome-wide transgenic RNAi library for conditional gene inactivation in Drosophila. Nature 448, 151–156.

Edwards, A., et al., 2011. Combinatorial effect of maytansinol and radiation in Drosophila and human cancer cells. Dis. Model. Mech. 4, 496–503.
Ekinci, F.J., Shea, T.B., 1999. Hyperactivation of mitogen-activated protein kinase increases phospho-tau immunoreactivity within human neuroblastoma: additive and synergistic influence of alteration of additional kinase activities. Cell. Mol. Neurobiol. 19, 249–260.
Feijoo, C., et al., 2005. Evidence that phosphorylation of the microtubule-associated protein tau by SAPK4/p38delta at Thr50 promotes microtubule assembly. J. Cell Sci. 118, 397–408.
Freeman, M., 1996. Reiterative use of the EGF receptor triggers differentiation of all cell types in the Drosophila eye. Cell 87, 651–660.
Fujita, K., et al., 2018. Targeting Tyro3 ameliorates a model of PGRN-mutant FTLD-TDP via tau-mediated synaptic pathology. Nat. Commun. 9, 433.
Greenwood, J.A., et al., 1994. Casein kinase II preferentially phosphorylates human tau isoforms containing an amino-terminal insert. Identification of threonine 39 as the primary phosphate acceptor. J. Biol. Chem. 269, 4373–4380.
Guise, S., et al., 2001. Hyperphosphorylation of tau is mediated by ERK activation during anticancer drug-induced apoptosis in neuroblastoma cells. J. Neurosci. Res. 63, 257–267.
Han, Z., et al., 2000. The staurosporine analog, Ro-31-8220, induces apoptosis independently of its ability to inhibit protein kinase C. Cell Death Differ. 7, 521–530.
Hanger, D.P., et al., 2009. Tau phosphorylation: the therapeutic challenge for neurodegenerative disease. Trends Mol. Med. 15, 112–119.
Hemstrom, T.H., et al., 2005. PKC 412 sensitizes U1810 non-small cell lung cancer cells to DNA damage. Exp. Cell Res. 305, 200–213.
Hoover, B.R., et al., 2010. Tau mislocalization to dendritic spines mediates synaptic dysfunction independently of neurodegeneration. Neuron 68, 1067–1081.
Hoshi, N., et al., 2010. Interaction with AKAP79 modifies the cellular pharmacology of PKC. Mol. Cell 37, 541–550.
Isagawa, T., et al., 2000. Dual effects of PKNalpha and protein kinase C on phosphorylation of tau protein by glycogen synthase kinase-3beta. Biochem. Biophys. Res. Commun. 273, 209–212.
Jackson, G.R., et al., 2002. Human wild-type tau interacts with wingless pathway components and produces neurofibrillary pathology in Drosophila. Neuron 34, 509–519.
Jensen, T.E., et al., 2009. Knockout of the predominant conventional PKC isoform, PKCalpha, in mouse skeletal muscle does not affect contraction-stimulated glucose uptake. Am. J. Physiol. Endocrinol. Metab. 297, E340–E348.
Joseph, B., et al., 2002. Mitochondrial dysfunction is an essential step for killing of non-small cell lung carcinomas resistant to conventional treatment. Oncogene 21, 65–77.
Kang, H.-L., et al., 2002. Life extension in Drosophila by feeding a drug. Proc. Natl. Acad. Sci. 99, 838–843.
Kanno, T., et al., 2014. Hyperphosphorylation of tau at Ser396 occurs in the much earlier stage than appearance of learning and memory disorders in 5XFAD mice. Behav. Brain Res. 274, 302–306.
Karsten, S.L., et al., 2006. A genomic screen for modifiers of tauopathy identifies puromycin-sensitive aminopeptidase as an inhibitor of tau-induced neurodegeneration. Neuron 51, 549–560.
Kaun, K.R., et al., 2011. A Drosophila model for alcohol reward. Nat. Neurosci. 14, 612–619.
Khurana, V., et al., 2006. TOR-mediated cell-cycle activation causes neurodegeneration in a Drosophila tauopathy model. Curr. Biol. 16, 230–241.
Lin, D.M., Goodman, C.S., 1994. Ectopic and increased expression of Fasciclin II alters motoneuron growth cone guidance. Neuron 13, 507–523.
Lopes, S., et al., 2016. Tau protein is essential for stress-induced brain pathology. Proc. Natl. Acad. Sci. 113, E3755.
Lucke-Wold, B.P., et al., 2015. Bryostatin-1 restores blood brain barrier integrity following blast-induced traumatic brain injury. Mol. Neurobiol. 52, 1119–1134.
Marsh, J.L., Thompson, L.M., 2006. Drosophila in the study of neurodegenerative disease. Neuron 52, 169–178.
Mayati, A., et al., 2015. Protein kinase C-independent inhibition of organic cation transporter 1 activity by the bisindolylmaleimide Ro 31-8220. PLoS ONE 10, e0144667.
Mayati, A., et al., 2017. Protein kinases C-mediated regulations of drug transporter activity, localization and expression. Int. J. Mol. Sci. 18.
McBride, S.M., et al., 2005. Pharmacological rescue of synaptic plasticity, courtship behavior, and mushroom body defects in a Drosophila model of fragile X syndrome. Neuron 45, 753–764.
Mochly-Rosen, D., et al., 2012. Protein kinase C, an elusive therapeutic target? Nat. Rev. Drug Discov. 11, 937–957.
Nelson, T.J., et al., 2017. Bryostatin effects on cognitive function and PKCvarepsilon in Alzheimer's disease phase IIa and expanded access trials. J. Alzheimers Dis. 58, 521–535.
Nikkel, A.L., et al., 2012. The novel calpain inhibitor A-705253 prevents stress-induced tau hyperphosphorylation in vitro and in vivo. Neuropharmacology 63, 606–612.
Nishimura, I., et al., 2004. PAR-1 kinase plays an initiator role in a temporally ordered phosphorylation process that confers tau toxicity in Drosophila. Cell 116, 671–682.
Okamoto, Y., Shikano, S., 2017. Differential phosphorylation signals control endocytosis of GPR15. Mol. Biol. Cell 28, 2267–2281.
Ollmann, M., et al., 2000. Drosophila p53 is a structural and functional homolog of the tumor suppressor p53. Cell 101, 91–101.
Ouseph, M.M., et al., 2015. Autophagy is induced upon platelet activation and is essential for hemostasis and thrombosis. Blood 126, 1224–1233.
Ozcelik, S., et al., 2013. Rapamycin attenuates the progression of tau pathology in P301S tau transgenic mice. PLoS ONE 8, e62459.
Pandey, U.B., Nichols, C.D., 2011. Human disease models in Drosophila melanogaster and the role of the Fly in therapeutic drug discovery. Pharmacol. Rev. 63, 411–436.
Papanikolopoulou, K., Skoulakis, E.M., 2015. Temporally distinct phosphorylations differentiate tau-dependent learning deficits and premature mortality in Drosophila. Hum. Mol. Genet. 24, 2065–2077.
Patrick, G.N., et al., 1999. Conversion of p35 to p25 deregulates Cdk5 activity and promotes neurodegeneration. Nature 402, 615–622.
Pearce, L.R., et al., 2010. The nuts and bolts of AGC protein kinases. Nat. Rev. Mol. Cell Biol. 11, 9–22.
Pierchala, B.A., et al., 2004. Nerve growth factor promotes the survival of sympathetic neurons through the cooperative function of the protein kinase C and phosphatidylinositol 3-kinase pathways. J. Biol. Chem. 279, 27986–27993.
Reynolds, C.H., et al., 1997. Stress-activated protein kinase/c-Jun N-terminal kinase phosphorylates tau protein. J. Neurochem. 68, 1736–1744.
Robey, R.W., et al., 2007. Inhibition of ABCG2-mediated transport by protein kinase inhibitors with a bisindolylmaleimide or indolocarbazole structure. Mol. Cancer Ther. 6, 1877–1885.
Robinow, S., White, K., 1988. The locus elav of Drosophila melanogaster is expressed in neurons at all developmental stages. Dev. Biol. 126, 294–303.
Shen, M.-Y., et al., 2008. Expression of amyloid beta peptide in human platelets: pivotal role of the phospholipase Cγ2-protein kinase C pathway in platelet activation. Pharmacol. Res. 57, 151–158.
Shi, H.B., et al., 2015. Alzheimer disease and cancer risk: a meta-analysis. J. Cancer Res. Clin. Oncol. 141, 485–494.
Shulman, J.M., Feany, M.B., 2003. Genetic modifiers of tauopathy in Drosophila. Genetics 165, 1233–1242.
Standaert, M.L., et al., 1999. RO 31-8220 activates c-Jun N-terminal kinase and glycogen synthase in rat adipocytes and L6 myotubes. Comparison to actions of insulin. Endocrinology 140, 2145–2151.
Szallasi, Z., et al., 1994. Differential regulation of protein kinase C isozymes by bryostatin 1 and phorbol 12-myristate 13-acetate in NIH 3T3 fibroblasts. J. Biol. Chem. 269, 2118–2124.
Tagawa, K., et al., 2015. Comprehensive phosphoproteome analysis unravels the core signaling network that initiates the earliest synapse pathology in preclinical Alzheimer's disease brain. Hum. Mol. Genet. 24, 540–558.
Talboom, J.S., et al., 2015. The mammalian target of rapamycin at the crossroad between cognitive aging and Alzheimer's disease. Npj Aging Mech. Disease. 1, 15008.
Terwel, D., et al., 2005. Changed conformation of mutant tau-P301L underlies the moribund tauopathy, absent in progressive, nonlethal axonopathy of tau-4R/2N transgenic mice. J. Biol. Chem. 280, 3963–3973.
Thomassen, M., et al., 2011. Protein kinase Calpha activity is important for contraction-induced FXYD1 phosphorylation in skeletal muscle. Am. J. Phys. Regul. Integr. Comp. Phys. 301, R1808–R1814.
Tomizawa, K., et al., 2001. Tau-tubulin kinase phosphorylates tau at Ser-208 and Ser-210, sites found in paired helical filament-tau. FEBS Lett. 492, 221–227.
Trinczek, B., et al., 2004. MARK4 is a novel microtubule-associated proteins/microtubule affinity-regulating kinase that binds to the cellular microtubule network and to centrosomes. J. Biol. Chem. 279, 5915–5923.
Vissers, J.H., et al., 2016. A Drosophila RNAi library modulates hippo pathway-dependent tissue growth. Nat. Commun. 7, 10368.
Wittmann, C.W., et al., 2001. Tauopathy in Drosophila: neurodegeneration without neurofibrillary tangles. Science 293, 711–714.
Yeo, E.J., et al., 1997. Dissociation of tyrosine phosphorylation and activation of phosphoinositide phospholipase C induced by the protein kinase C inhibitor Ro-31-8220 in Swiss 3T3 cells treated with platelet-derived growth factor. Biochim. Biophys. Acta 1356, 308–320.